On eustatic sea level history: Last Glacial Maximum to Holocene

W.R. Peltier*

Department of Physics, University of Toronto, 60 St. George Street, Toronto, Ont., Canada M5S 1A7

Abstract

This paper addresses the question of the magnitude and time dependence of the globally averaged (eustatic) rise of sea level that occurred subsequent to the time of Last Glacial Maximum (LGM) at approximately 21,000 calendar years before present. Through the analysis of relative sea level (RSL) histories predicted by a realistic mass conserving and gravitationally self-consistent theory of postglacial sea level change, it is demonstrated that there are preferred oceanic locations at which this eustatic function is well approximated by local sea level history. One such location is the Island of Barbados in the Caribbean Sea, a site from which a coral based record exists that extends from mid-Holocene to LGM. Because of the sea level ambiguity that is inherent to coral based records, however, it is important that the global ice-equivalent eustatic sea level curve inferred on the basis of the Barbados data be tested against observations at other locations from which similarly extensive records are also available but which are derived on the basis of sea level indicators which are not subject to the ambiguities inherent to corals. It is shown that, when the eustatic function employed in the global theoretical model is tuned so as to enable the model to fit the Barbados observations, where the maximum relative sea level (RSL) depression is assumed to be near 120 m, then the theory misfits the record from the Sunda Shelf in the Indonesian Archipelago as well as the record from J. Bonaparte Gulf in northern Australia. Both of these recently published records appear to constrain the LGM low stand of RSL to a value above 120 m. The implications of these results for interpretation of the long coral derived records from the Huon Peninsula of Papua, New Guinea and the island of Tahiti are also discussed. © 2001 Published by Elsevier Science Ltd.

1. Introduction

Since the eustatic (globally averaged) rise of sea level that occurred subsequent to last glacial maximum (LGM) is determined by the total mass of land based ice that melted during the transition from full glacial to Holocene conditions, it is clearly critical to the success of the EPILOG project of PAGES that the best possible estimate of this "eustatic function" of the deglaciation event be obtained. If for no other reason, this is because the thicknesses of the continental ice-sheets that existed at LGM are strongly constrained by the net eustatic rise which their melting induced (e.g. Peltier, 1994, 1996). These thicknesses in turn determine the ice-sheet contributions to planetary paleotopography from LGM onwards (op. cit.), a field which clearly exerts strong influence on the climate of the LGM epoch that is inferred on the basis

of Atmosphere–Ocean General Circulation Model reconstructions (e.g. see Vettoretti et al., 2000; Peltier and Solheim, 2001 for recent examples). In the very recent past, a large number of such reconstructions have been intercompared in the context of the international Paleoclimate Model Intercomparison Project (PMIP), a recent discussion of the results from which has been presented in Pinot et al. (1999), see also Vettoretti et al. (2000). These LGM climate reconstructions have all employed the paleotopography and land-sea mask based upon the ICE-4G (VM2) model of Peltier (1994, 1996) which is characterized by an ice-equivalent eustatic function for which the net LGM to Holocene eustatic sea level rise is 117.8 m (see Fig. 37 of Peltier, 1998a) when the contribution to the eustatic function due to the influence of "implicit ice" (Peltier, 1998b) is properly taken into account.

The net eustatic rise of 117.8 m delivered by the ICE-4G (VM2) model of postglacial relative sea level history is insignificantly different from the nominal value of 120 m that has been advocated for some time on the

*Tel.: +1-416-978-2938; fax: +1-416-978-8905.

E-mail address: peltier@atmosp.physics.utoronto.ca (W.R. Peltier).

basis of estimates derived from calibration of the deep sea oxygen isotopic record (e.g. see Shackleton, 2000, Fig. 4b), although the relation between benthic $\delta^{18}O$ and eustatic sea level may be somewhat imprecise. However, the value of approximately 120 m for the eustatic sea level depression has also been suggested on the basis of the coral derived record from the island of Barbados (Fairbanks, 1989; Bard et al., 1990a, b), although no argument was available to these authors as to why the local RSL record from Barbados should provide a good approximation to eustatic sea level history. It was simply assumed that this should be the case, an assumption that the analyses to be presented herein will demonstrate to have been fully justified. I had previously raised the question (see Peltier, 1995 commenting in response to Edwards, 1995) as to whether the Barbados record should in fact be expected to provide an accurate approximation to the LGM-to-Holocene eustatic function. It has been possible to resolve this important issue only by recognition of the role played by "implicit ice" (Peltier, 1998b) in the version of the global theory of postglacial RSL history that fully incorporates the influence of time variations in the coastline (Peltier, 1994). In recently published commentary by members of the EPILOG Program, the legitimacy of the ICE-4G (VM2) estimate of the eustatic function has been seriously questioned (e.g. Clark and Mix, 2000). The primary basis for the suggestion that the ICE-4G (VM2) model could be significantly in error is based on two lines of argument. The first of these derives from the effort by Fleming et al. (1998) to infer the glacial to interglacial eustatic function based upon analysis of a variety of records from what I have referred to in the past as the "far-field" of the ice-sheets. Although the Fleming et al. (1998) eustatic function is characterized by a net eustatic rise of ~ 120 m, it has a number of characteristics that make it questionable on a-priori grounds, including (1) that it does not contain the intense meltwater pulse 1a (mwp1a) feature which is so prominent in the Barbados record of Fairbanks (1989), and (2) it does contain a significant late Holocene "melting tail" of a eustatic strength that the authors believe could be as high as $0.5\,\mathrm{mm\,yr^{-1}}$. The second line of analysis that has led to questioning of the ICE-4G (VM2) reconstruction is connected with the more recent paper by Yokoyama et al. (2000) in which, on the basis of a pre-Holocene RSL reconstruction derived from micropaleontological indicators of sea level in sediments from the continental shelf in the J. Bonaparte Gulf of Northern Australia, the authors have suggested the existence of a sharp rise of eustatic sea level from a low stand of ~ 135 m at LGM to a new level ~ 120 m below present at 19,000 calendar years before present. If this additional 15 m of eustatic rise were correct (the authors specifically preferred eustatic rise at

this time is closer to 13.5 m) it would clearly have significant implications insofar as maximum thicknesses of the LGM ice sheets are concerned as these were inferred in Peltier (1994, 1996, 1998b) using the viscoelastic theory for glacial isostatic adjustment to "weigh" these structures using observed rebound amplitudes to infer LGM ice-thickness. As I will argue in what follows, both of these lines of argument that have suggested significant error in the ICE-4G reconstruction are seriously flawed. As I will also point out, however, there do exist valid arguments that could be construed to imply a net LGM to present eustatic rise in excess of the nominal value of ~ 120 m that is characteristic of ICE-4G.

Since these arguments rely significantly upon the structure of the global theory of the glacial isostatic adjustment and postglacial sea level change process that my colleagues and students and I have developed, Section 2 to follow reviews those aspects of the theory that are crucial to understanding the connection between the eustatic function of the model and local RSL histories. This connection has never been explored in detail in any previous publication. In Section 3 I demonstrate explicitly, by tuning the global model of deglaciation so as to enable the theory to predict the RSL history observed at Barbados, that the local RSL history at Barbados is an excellent approximation to the eustatic function of the model that is employed to predict RSL history globally although the data from Barbados do not accurately record the LGM lowstand. Section 4 addresses the question of the global predictive capacity of the model that has been tuned in this fashion by comparing theoretical RSL history predictions with RSL observations from the Sunda Shelf (Hanebuth et al., 2000), J. Bonaparte Gulf (Yokoyama et al., 2000), and the Argentine Shelf (Guilderson et al., 2000). Also discussed are the long coral based RSL records from the Huon Peninsula (e.g. Chappell et al., 1998) and from Tahiti (Bard et al., 1996) as well as an assortment of other records from a number of equatorial Pacific islands. Conclusions are offered in Section 5.

2. The global theory of glacial isostatic adjustment: implications for eustatic sea level history

The modern global theory of glacial isostatic adjustment and postglacial relative sea level history originated in a series of papers published in the mid-1970's (Peltier, 1974; Peltier and Andrews, 1976; Farrell and Clark, 1976; Peltier, 1976; Clark et al., 1978; Peltier et al., 1978). On the basis of the detailed analyses presented in these papers it became possible for the first time to predict the history of relative sea level that should be

observed at any point on the Earth's surface and to compare these predictions with reliably dated records of the history of relative sea level change subsequent to LGM wherever these were available. Such predictions were made by solving an integral equation that I have come to call the "Sea Level Equation (SLE)". This equation, which is a construct of first order perturbation theory, may be written schematically for the variation of relative sea level $S(\theta, \lambda, t)$ as:

$$S(\theta, \lambda, t) = C(\theta, \lambda, t)[G(\theta, \lambda, t) - R(\theta, \lambda, t)], \quad (1)$$

in which C is the "ocean function" which equals unity over the global ocean and zero elsewhere, G is the glacial isostasy induced perturbation to the geoid of classical geodesy which is a surface of constant gravitational potential that is coincident with mean sea level over the oceans, and R is the perturbation to the local radius of the solid earth. To first order in perturbation theory, G and R may be explicitly computed (Peltier, 1974; Peltier and Andrews, 1976) once one knows the time dependent surface mass load to which the planet is subjected as a consequence of the glaciation–deglaciation process. This surface load has both ice and water components and so has a composite form that may be written:

$$L(\theta, \lambda, t) = \rho_I I(\theta, \lambda, t) + \rho_w S(\theta, \lambda, t), \quad (2)$$

in which ρ_I and ρ_w are the densities of ice and water, respectively and in which I and S are the variations of the ice and water thicknesses respectively. The variation of water thickness (bathymetry) is of course just the variation of relative sea level S, as stated above. The most complete form of the SLE that is currently available is:

$$
\begin{aligned}
S(\theta, \lambda, t) = C(\theta, \lambda, t)&\left[\int_{-\infty}^{t} dt' \int\int_{\Omega} d\Omega'[L(\theta', \lambda', t')\right.\\
&\times \left\{\frac{\phi^L(\gamma, t - t')}{g} - \Gamma^L(\gamma, t - t')\right\}\\
&\left.+ \Psi^R(\theta', \lambda', t')G_\phi^T(\gamma, t - t')] + \frac{\Delta\Phi(t)}{g}\right]\\
= C[T_o &+ \Delta\Phi(t)/g]. \quad (3)
\end{aligned}
$$

In Eq. (3) the functions ϕ^L and Γ^L are Green functions for the perturbations of gravitational potential and radius for the surface-mass-load boundary value problem that were first computed for a radially stratified viscoelastic Earth by Peltier and Andrews (1976) and Peltier (1974) respectively and λ is the difference in position between source point (θ', λ') and field point (θ, λ). The functions Ψ^R are and G_ϕ^T are fully described in Peltier (1998a, 1999) following Dahlen (1976) and are those required to represent the impact of the changing rotational state of the planet on relative sea level history. Finally, the function $\Delta\Phi(t)/g$ in Eq. (3) is critical in the context of the present paper.

It describes a time dependent but space independent correction to the instantaneous space and time dependent sea level height prediction, determined by the triple convolution integral T_o in (3), that must be added to the RHS of (3) in order to ensure that the predictions of the theory are consistent with the principle of conservation of mass. The ocean function C in (3), which was assumed to be constant in all of the early work cited above, is in general time dependent so that the surface area of the ocean $A(t)$ is also time dependent. The time dependence of C may be computed using the global "topographically self consistent" method for solving (3) described in Peltier (1994) and it is in the context of the application of this algorithm that the concept of "implicit ice", to be discussed further below, naturally arises.

Referring first to the paper by Clark et al. (1978) it will be clear from their Eq. (1) that the term written as $\Delta\Phi(t)/g$ in my Eq. (3) is identical to their sum of terms $-k_E(t) - k_c(t)$. Since the globally averaged (eustatic) rise of sea level must be such that:

$$\int_{A(t)} \rho_w S(\theta, \lambda, t)\, d\Omega = M_I(t) = -\rho_I \int_{-\infty}^{t} \frac{dV_I}{dt} dt, \quad (4)$$

where $M_I(t)$ is the total mass lost by the melting of ice by time t, V_I is ice volume, and $A(t)$ is the time varying area of the ocean basins, it follows that:

$$M_I(t) = \rho_w \int\int_{A(t)} T_o d\Omega + \rho_w \int\int_{A(t)} \frac{\Delta\Phi(t)}{g} d\Omega,$$

$$\text{or,} \quad \frac{\Delta\Phi(t)}{g} = \frac{M_I(t)}{\rho_w A(t)} - \frac{1}{A(t)} \int\int_{A(t)} T_o\, d\Omega. \quad (5)$$

The factor $\Delta\Phi(t)/g$ is the factor that must be added to the right-hand side of (3) in order to ensure that the model of RSL history conserves mass. Now the first term on the right-hand side of (5) is just the ice-equivalent eustatic sea level history, $S_{eus}(t)$ say, thus:

$$S_{eus}(t) = \frac{M_I(t)}{\rho_w A(t)} = \frac{-\rho_I(V_I(t) - V_I(o))}{\rho_w A(t)}, \quad (6)$$

where $V_I(t)$ is the total volume of ice at time t and $V_I(0)$ is the larger volume of ice that existed earlier at the onset of deglaciation at LGM, which I have assumed to be the zero of time, prior to which I will assume for present purposes the system to have been in isostatic equilibrium. $S_{eus}(t)$ is therefore derived solely on the basis of the knowledge of the mass of ice that has melted by time t, namely $M_I(t)$, the density of water ρ_w, and the area of the ocean basins at time t, namely $A(t)$. Substituting Eq. (5) into (3), we then have:

$$S(\theta, \lambda, t) = C[T_o - \langle T_o \rangle + S_{eus}(t)]. \quad (7)$$

in which

$$\langle T_o \rangle = \frac{1}{A_o(t)} \int\int_{A(t)} T_o\, d\Omega \quad (8)$$

is the average value of the triple convolution integral in (3) over the surface of the oceans at time t. It therefore follows that the local RSL history $S(\theta, \lambda, t)$ will be identical to the eustatic sea level history $S_{eus}(t)$ if and only if

$$T_o = \langle T_o \rangle. \tag{9}$$

Once more comparing Eq. (7) with Eq. (1) in Clark et al. (1978), it will be clear that their $-k_E(t) = S_{eus}(t)$ whereas their $k_c = \langle T_o \rangle$. A point that will be of primary concern to us here is where we should look on the surface of the Earth to find sites at which $T_o = \langle T_o \rangle$ so that $S(\theta, \lambda, t) = S_{eus}(t)$.

A crucial issue that immediately arises, when the impact of time-dependent ocean function is included in the theory, however, concerns the role of "implicit ice" first recognized in Peltier (1998b). When significant changes in C occur, as when the Hudson Bay, the Gulf of Bothnia and the Barents and Kara Seas become reconnected to the global ocean as the grounded continental ice-sheets that initially covered these regions disintegrate, effects occur that are not properly represented by Eq. (7). They are simply too large. As discussed in Peltier (1998b), these effects act in such a way as to be equivalent, on the surface of the deglaciating and deforming Earth, to the melting of an additional amount of ice from the glaciated portion of the surface which is later inundated by the sea. In computing the eustatic function for a given model of deglaciation and postglacial RSL change, this "implicit ice" must be included in the function $M_I(t)$ in Eq. (4) together with the time dependence of the surface area of the oceans. The expression for $S_{eus}(t)$ then takes the general form:

$$S_{eus}(t) = \frac{M_I^{ex}(t) + M_I^{im}(t)}{\rho_w A(t)}. \tag{10}$$

The purpose of this paper is to better understand the relationship between the $S_{eus}(t)$ which includes the contribution due to "implicit ice", for acceptable models of the LGM to Holocene deglaciation event, and the RSL records $S(\theta, \lambda, t)$ observed at specific locations with latitude θ and longitude λ in the far field of the ice-sheets.

Since the necessity of introducing the concept of "implicit ice" derives from application of the algorithm of Peltier (1994) to compute the time dependence of the ocean function $C(\theta, \lambda, t)$, it will prove important to further discuss the details of this algorithm here. In the analysis procedure that has been developed to include this influence on the theory of postglacial RSL history, the effect is introduced in an iterative fashion. To understand how this works, it is important to note that the sea level Eq. (3) is a construct of first order perturbation theory. Solution of this integral equation constitutes a prediction of the global history of

"relative" sea level change that is induced by a particular model of the deglaciation process, a history which is "relative" to the deforming surface of the solid Earth but in which the actual complex surface topography is unspecified and therefore arbitrary. The arbitrariness of this datum may be usefully exploited so as to construct a solution that I refer to as being "topographically self-consistent" in which the datum relative to which sea level variations are described is explicitly defined as being the complex real topography of the surface of the solid Earth. Given a solution $S(\theta, \lambda, t)$ to (3), determined at first on the basis of the assumption that the ocean function C is identically equal to its present form, we first construct a new field $S_{TOP}(\theta, \lambda)$ such that:

$$S(\theta, \lambda, t_p) + S_{TOP}(\theta, \lambda) = TOP(\theta, \lambda, t_p) \tag{11}$$

in which $TOP(\theta, \lambda, t_p)$ is the present day topography of the Earth with respect to the present day (t_p) sea level. For the field TOP I have continued to employ the ETOPO5 database. Given the S_{TOP} that satisfies Eq. (11), it will then be clear that we may estimate the topography of the rocky part of the planet relative to sea level at any time in the past by simply computing:

$$TOP(\theta, \lambda, t) = S(\theta, \lambda, t) + [TOP(\theta, \lambda, t_p) - S(\theta, \lambda, t_p)]. \tag{12}$$

From (12) then follows an estimate for time-dependent paleotopography PTOP by simply adding to TOP the thickness of local continental ice to obtain:

$$PTOP(\theta, \lambda, t) = TOP(\theta, \lambda, t) + I(\theta, \lambda, t), \tag{13}$$

where the ice-thickness $I(\theta, \lambda, t)$ includes both explicit and implicit parts, the latter to be more fully discussed in succeeding paragraphs. Eq. (13) now provides a basis for computing the time dependence of the ocean function $C(\theta, \lambda, t)$. We simply note that where PTOP is negative there is ocean, whereas where PTOP is positive there is (perhaps ice-covered) land. This determines a first approximation to the time dependence of $C(\theta, \lambda, t)$ which we denote by C^1. To improve this first approximation we next solve Eq. (3) once more, assuming $C = C^1$, and follow the same procedure outlined above to obtain a second approximation C^2. Typically this iterative process converges to a sufficiently accurate solution for the time dependent ocean function within 3 iterations.

In order to be specific concerning the spatial and temporal distribution, as well as the amount, of "implicit-ice" that will be operative in the models of postglacial sea level history to be discussed in what follows, due to the use of the above described iterative procedure to determine the time dependence of the ocean function, it will prove useful to also revisit the algorithm employed to compute this quantity

and to further explain in physical terms why it is necessary. As discussed above, the necessity of introducing the concept of "implicit ice" follows from application of this topographically self-consistent methodology to compute the evolving position of the coastline and thus the evolving surface area of the oceans. Whether or not rotational feedback is included (Eq. (3)) in the SLE, application of the algorithm of Peltier (1994) to determine the time dependence of the ocean function introduces strong effects into the theoretical solution determined by solving the SLE. For this reason the ice-load component $I(\theta, \lambda, t)$ of the total surface load $L(\theta, \lambda, t)$ in Eq. (2), which is chosen in the process of tuning the model so as to enable it to fit the small subset of observational data employed for this purpose, becomes an "effective" history of deglaciation. Since this effective load that is a required input to the SLE is chosen so that the solution of this equation accurately fits the data employed in the tuning process, it will be clear that the question immediately arises as to the connection between this "explicit" history $I_{ex}(\theta, \lambda, t)$ that is employed as input to (3) and the "actual" load that must have been removed, the possibility of a difference $I_{im}(\theta, \lambda, t)$, to which I refer as "implicit ice", existing because of the action of the influence of the large changes in $C(\theta, \lambda, t)$ that occur when regions like the Hudson Bay, which were originally ice-covered, become connected to the global ocean. That such a difference must exist was first strongly suggested by Fig. 3b of Peltier (1994) in which the total eustatic rise of approximately 120 m observed at Barbados was shown to be significantly greater than the 105.2 m eustatic rise expected on the basis of the amount of land ice I_{ex} that had to be explicitly melted in order to induce the ~ 120 m rise of RSL observed at Barbados. In response to the comment by Edwards (1995), Peltier (1995) suggested that the problem could lie in the difference between the RSL history at Barbados and ice-equivalent eustatic sea level history. How this issue was finally resolved in Peltier (1998a-c) will be discussed next in detail (some readers may be interested to know that the complete algorithm that is now employed to compute this "implicit" component of the ice-load had been fully developed by the summer of 1997).

Analysis of the output of the solution to the SLE which employs the "topographically self-consistent" methodology to incorporate the time dependence of C, shows that, at a point on the surface of the Earth which is initially ice-covered (say within Hudson Bay) but which at some later time becomes connected to the ocean, the time series for $S(\theta, \lambda, t)$ at this point is predicted to have the form

$$S(\theta, \lambda, t) = \Delta S(\theta, \lambda)H(t - t_D) + S'(\theta, \lambda, t), \qquad (14)$$

in which t_D is the time of deglaciation when the sea first occupies the point in question, $\Delta S < 0$ is an instantaneous fall of relative sea level that is delivered by the solution of the SLE when reconnection to the ocean occurs, H is the Heaviside step function and $S'(\theta, \lambda, t)$ is a function which vanishes at $t = t_D$ but which thereafter decreases with time so as to represent the continuing loss of water that thereafter occurs from the initially ice-covered region as postglacial rebound of the crust continues. The abrupt fall of relative sea level that occurs at $t = t_D$, in the amount ΔS, occurs because there is a difference in gravitational potential at that time between the surface of the exterior ocean and the point in question. Through Eq. (2) this loss of surface water load from the initially ice-covered region, where no water initially exists (!), clearly exerts a negative load on the surface, thereby increasing the isostatic response to load removal. This is entirely equivalent to, and must clearly be described as, the removal of an additional amount of ice such that the net load removed from the initially ice-covered portion of the surface becomes:

$$L = \rho_I \left[I_{ex}(\theta, \lambda, t) + \frac{\rho_w}{\rho_I} \Delta S(\theta, \lambda) H(t - t_D) \right]$$
$$= \rho_I [I_{ex}(\theta, \lambda, t) + I_{im}^I(\theta, \lambda, t)]. \qquad (15)$$

Because mass is conserved in the SLE, the additional ice load I_{im}^1 that is removed (as water) from the initially ice-covered region is of course delivered to the external ocean basins. A second contribution to the net "implicit ice" which acts in concert with I_{ex} is connected to the term S' in Eq. (14). Because the SLE is a construct of first order perturbation theory, it should be clear that when initially ice-covered land comes to be inundated by the sea as a consequence of the time dependence of C, the theory does not explicitly compute the amount of water that subsequently covers the "new" surface area of the ocean (although the SLE could be adjusted so that it did so). Rather it is simply assumed that the region is covered by water of unspecified depth. However, we may accurately compute the amount of water that must have initially covered the region by simply computing the predicted present day altitude of the marine limit (ML) and adding to this the present day (time $= t_p$) depth H of the water (determined, say, using the ETOPO5 data set) in this region. Since this water must also have been produced by melting ice, this delivers a second contribution to implicit ice that we may represent as

$$I_{im}^2(\theta, \lambda, t) = \frac{\rho_w}{\rho_I}(ML(\theta, \lambda, t \leqslant t_D) + H(\theta, \lambda, t_p)) \qquad (16)$$

The term M_I^{im} in Eq. (10) is therefore, explicitly:

$$M_I^{im} = -\rho_I \int_{-\infty}^{t} \frac{dV_I^{im}}{dt} dt \qquad (17)$$

in which $V_1^{im}(t)$ is the time dependent volume of implicit ice. Graphical depictions of the spatial distribution of $I_{im} = I_{im}^1 + I_{im}^2$ at LGM will be provided in the next section. When the influence of implicit ice is included in the analysis, because the time dependence of C is fully taken into account, Eq. (7) must be modified appropriately to the form:

$$S(\theta, \lambda, t) = C[T_o - \langle T_o \rangle + S_{eus}(t) - S_{eus}^{im}(t)] \qquad (18)$$

It is therefore clear from (18) that a local relative sea level history $S(\theta, \lambda, t)$ will equal the ice equivalent eustatic function only where $T_o - \langle T_o \rangle = S_{eus}^{im}(t)$. Here, as in (10), $S_{eus}(t) = S_{eus}^{ex}(t) + S_{eus}^{im}(t)$ is the ice-equivalent eustatic sea level history. Because $S_{eus}^{im}(t)$ is both added and subtracted from the right-hand side of (18), its inclusion has no impact at all upon the theoretical prediction of relative sea level history as pointed out in Peltier (1998b). However, it must be included in this way if by $S_{eus}(t)$ we are to continue to mean the ice-equivalent eustatic sea level history. What it does do is to modify the condition that must obtain in order that local RSL history equals eustatic RSL history. Eq. (18) has not been recorded previously and is central to the discussion to follow in the present paper. As will be clear on the basis of the above described details of the algorithms employed to determine $I_{im}^1(\theta, \lambda, t)$ and $I_{im}^2(\theta, \lambda, t)$, these quantities may be computed exactly in principle (i.e. given sufficiently high spatial and temporal resolution.

Additional but less apparent influences of the time dependence of C also occur in regions where initially exposed broad continental shelves become inundated by the sea but these effects are usually much less important than the "implicit ice" effect upon which I have focused herein. These additional influences will be discussed further in what follows and in greater detail elsewhere (Peltier and Drummond, 2001).

3. Tuning the global model and the connection between Barbados RSL history and ice-equivalent eustatic RSL history

In the construction of the ICE-4G (VM2) model of the global process of glacial isostatic adjustment, the primary data sets employed to control the total mass of ice that disappeared from the continents subsequent to LGM consisted, firstly, of the amplitudes of postglacial emergence of the land observed at sites that were once ice-covered, data which provide a strong constraint on local ice-thickness if an accurate model of the radial viscoelastic structure of the planet is available (see Peltier, 1996, 1998a, c for analyses which support the choice of the VM2 model as the preferred model for the radial viscoelastic structure) and if the timing of load removal is

well constrained by surface geomorphological observations such as those produced by Dyke and Prest (1987) for the Laurentian platform. Also employed as a primary constraint upon the ICE-4G (VM2) model was the U–Th dated RSL record from the island of Barbados in the Caribbean Sea (Fairbanks, 1989; Bard et al., 1990a, b). As previously mentioned, the ICE-4G deglaciation history was characterized by a net eustatic rise subsequent to LGM of 117.8 m, of which approximately 21.7 m was assumed to have been derived from the melting of Antarctic ice (see Fig. 37 of Peltier, 1998a). Since this assumption as to the amount of Antarctic melting is now widely believed to have been significantly greater than actually occurred (e.g. see Huybrechts, 1992 for early glaciological reconstructions and Huybrechts, 2001, this volume, for an update of his analyses), for present purposes I will focus on a slightly modified version of ICE-4G for which the individual geographical contributions to the net eustatic rise are shown in Fig. 1 (top). Also shown in Fig. 1 (bottom) is the prediction of the present day rate of RSL rise when this deglaciation model, in which Antarctica and Patagonia are collectively assumed to have contributed 17.6 m to the net eustatic rise, is employed together with a model of the radial viscoelastic structure in which the lithospheric thickness L is taken to be 90 km, somewhat smaller than the value of 120.7 km that characterized this feature in the VM2 model. The detailed rationale for exploring the influence of this reduction in lithospheric thickness, which is minor for most purposes, is provided in Peltier et al. (2001), a paper which is also commented upon in Shennan et al. (2001, this volume). The net ice-equivalent eustatic rise in this slightly modified model of deglaciation history, denoted by S_{eus} in Fig. 1 (top), is 113.5 m. The contribution to the net eustatic rise due to the "explicit ice" employed in the solution of the SLE for this model was 103.5 m and is denoted by the dashed line in the figure that is labelled S'_{eus}; the implicit component was therefore approximately 10 m. The individual North American (N), European (E), Antarctic + Patagonia (A) and Greenland (G) contributions to the net eustatic rise are also shown in this figure for both "explicit" and "explicit plus implicit" ice. Although it is now well understood that the Greenland component of this eustatic sea level history is excessive (Tarasov and Peltier, 2001), the overestimate of the Greenland contribution to $S_{eus}(t)$, by approximately 3 m, will not be of any importance for present purposes since the mass that would be missing if this overestimate were eliminated may simply be incorporated into the Laurentide Ice Sheet (LIS). It should be understood that by investigating the RSL predictions of a model in which the net eustatic rise has been reduced from that in the ICE-4G (VM2)
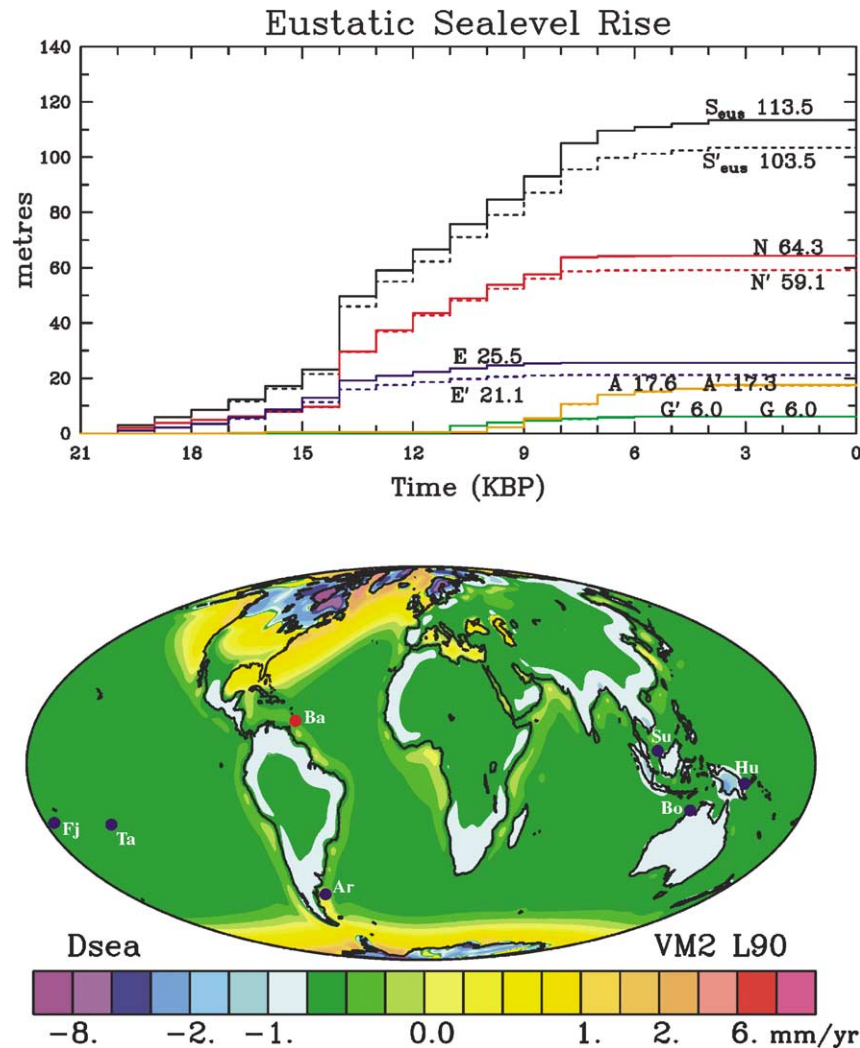
Fig. 1. (a) Ice equivalent eustatic sea level curves for the individual geographical regions in which LGM-to-Holocene deglaciation occurred according to the model to be primarily employed for the analyses discussed in this paper. The solid and dashed curves respectively correspond to the total and to the "explicit ice" derived components from G (Greenland), A (Antarctica), E (Eurasia) and N (North America). The sum of all these contributions defines the eustatic function of the deglaciation model which is labelled S_{eus}. The function S'_{eus} is the contribution to the eustatic function due to "explicit ice" alone, the "implicit ice" derived component being the difference between S_{eus} and S'_{eus}. (b) The model predicted present day rate of relative sea level rise that would be measured by the secular variation of sea level on a tide gauge. Also shown in this figure are the locations of the sites that are especially important for the purpose of this paper. The location of Barbados is labelled Ba in the figure and this site is employed to tune the model eustatic function. The remaining sites at the Huon Peninsula of Papua, New Guinea (Hu), Tahiti (Ta), Sunda Shelf (Su), Bonaparte Gulf (Bo) and the Argentine Shelf (Ar) are employed to verify the quality of the predictions of the model which is tuned to the Barbados record.

model, by approximately 4.3 m, I am not herein advocating the notion that the net eustatic rise in the ICE-4G model was excessive. In fact the analyses to follow will demonstrate that the 113.5 m net eustatic rise in the present model is a lower bound to that which actually characterized the glacial interglacial transition. Our best estimate for this important characteristic of LGM conditions will infact prove to be higher than 120 m, the increase to this level from the lower bound being easily absorbed by further modifications to the deglaciation history of North America and elsewhere.

Fig. 2 shows the implicit components of the LGM ice-cover of both the first and second kinds, I_{im}^1 and I_{im}^2 respectively, as well as the total I_{im} for the present model for both North America and Northwestern Europe. Comparing the results in these figures, in which the implicit components of the LGM ice cover are shown in terms of their thickness, to the equivalent results for ICE-4G (VM2) in Figs. 2 and 3 of Peltier (1998b), demonstrates that the differences in the spatial distributions between the results for these two models are minor as one would expect. There is, however, a significant difference
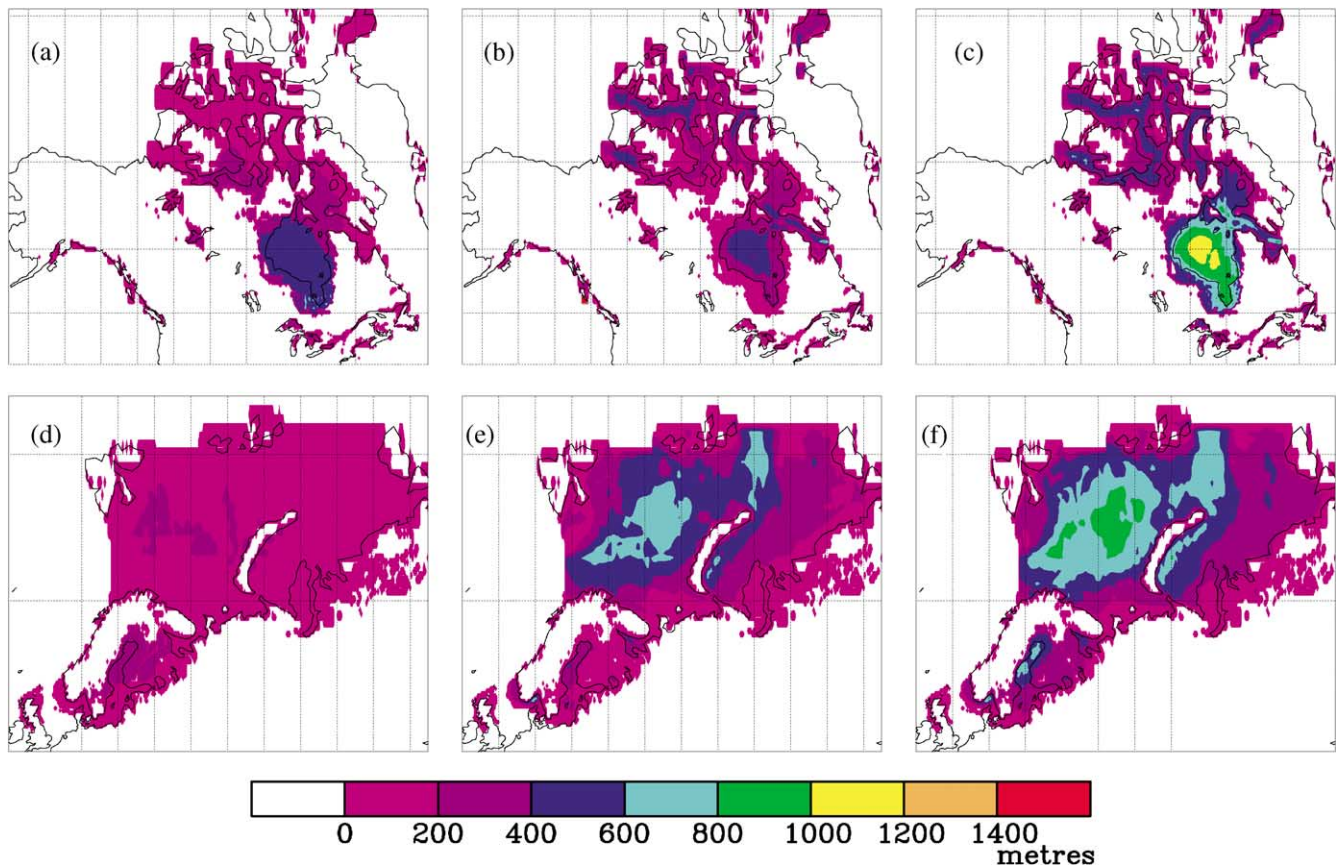
Fig. 2. (a) The LGM geographical distribution of the thickness of implicit ice of type 1, I_{im}^1 over North America, (b) the LGM geographical distribution of the thickness of implicit ice of type 2, I_{im}^2, over North America, (c) the LGM spatial distribution of total implicit over North America, (d–f) the same as (a–c) but for Northwestern Europe.

between the results shown here for thickness and the previous results which were shown in terms of topography relative to sea level, this difference being due to the influence of isostatic adjustment. Evident by inspection of Fig. 2 is the fact that there exists some highly localized "noise" in the computation of both I_{im}^1 and I_{im}^2 that arises due to the restricted spatial resolution of the analyses in regions in which the margins of the continental ice-sheets are specified as extending into deep water. The collective effect of this noise in the specification of I_{im}, however, is entirely negligible quantitatively.

The location of the island of Barbados in the Caribbean Sea is shown in Fig. 1 (bottom) where it is denoted Ba, as are the locations of other sites that will be important for the purpose of the discussion to follow, respectively Tahiti (Ta), The Huon Peninsula (Hu) of Papua New Guinea, the Fiji Islands (Fj), the Sunda Shelf (Su), J. Bonaparte Gulf (Bo), and the Argentine Shelf (Ar). Concerning the position of the key Barbados site, it is important to note that it is located beyond the trailing edge of the glacial forebulge, and therefore is well outboard of the

region along the US east coast within which there exists a strong impact upon postglacial RSL history due to the downward vertical motion of the solid Earth. This region of "glacial forebulge collapse" is clearly evident in Fig. 1 as the region outboard of the former location of the LIS in which relative sea levels are currently rising, due to the on-going influence of glacial isostatic adjustment of the solid Earth. Furthermore, because Barbados is an island location that is well offshore of the coast of Venezuela, it is not influenced significantly by the tilting of the surface of the solid Earth that is caused by the emplacement of the offshore water load due to the meltback of the continental ice-sheets. It is therefore plausibly a location at which the local RSL history might approximately satisfy the condition $T_o = \langle T_o \rangle + S_{eus}^{im}$ that is required in order that such a local sea level history be identical to the ice-equivalent eustatic sea level history.

That the Barbados RSL history should be essentially identical to ice-equivalent eustatic sea level history is demonstrated explicitly in Fig. 3 for the slightly modified version of the ICE-4G (VM2) model that

is under consideration herein. In this figure the coral based RSL estimates of Fairbanks (1989), corrected for the conventionally assumed rate of tectonic uplift of 0.34 mm per year, on the U–Th based calendar year timescale of Bard et al. (1990a, b), are plotted together with both the step-discontinuous model eustatic curve based upon Eq. (10) that is characteristic of the deglaciation history that is employed as input to the theoretical calculation, and the output of the sea level Eq. (18) which is shown as the smooth dashed curve (rotational feedback effects have been explicitly shown to be small, insofar as relative sea level history is concerned, in both Milne and Mitrovica, 1996 and Peltier, 1998a, 1999 and so I have not included this effect for the purpose of constructing Fig. 3; its influence will be discussed further below). In plotting the individual RSL observations at Barbados, the length of the vertically pointing error bars has been chosen so as to distinguish the measurements derived from the *Acropora palmata* species of coral from those based upon the *Porities* species, the former generally being restricted to a living depth within 6 m of sea level (in the modern ecology), whereas the latter may be found at considerably greater depth below the instantaneous level of the sea. Inspection of Fig. 3 in fact demonstrates that *Porities* is generally deeper in the water column at Barbados then *Acropora palmata* (Ap) by as much as 20 m (e.g. see the Porities sample whose age in calendar years is near 13,000 ka) and above which are found Ap samples of the same age at much shallower depth below present sea level.

Other features of the model fit to the Barbados data set are also important for present purposes. Note for example that in this reconstruction no attempt has been made to insert into the eustatic function of the model an equivalent to Fairbanks (1989) meltwater pulse 1b (mwp1b) event that is suggested by the coral derived measurements in the post Younger–Dryas age-range between 11 and 10 ka. This was included in the original ICE-4G (VM2) reconstruction and will be reinserted in the final form of the ICE-5G model that is currently under development. The meltwater pulse 1a (mwp1a) event, however, at approximately 14 ka, is as pronounced in the model (by design) as in the data. Note also that there is a dense cluster of dated *Acropora palmata* samples in the age range 16–19 ka which appear to strongly constrain eustatic sea level to a depth less than 110 m in this interval if we respect the depth of the shallowest sample in this duster. Beyond the age of 19 ka, however, and extending to LGM at approximately 21 ka, the only samples available are of the species *Porities*, the oldest of which have a calendar year age near 22 ka and are found at a d epth shallower than 135 m. The Barbados record
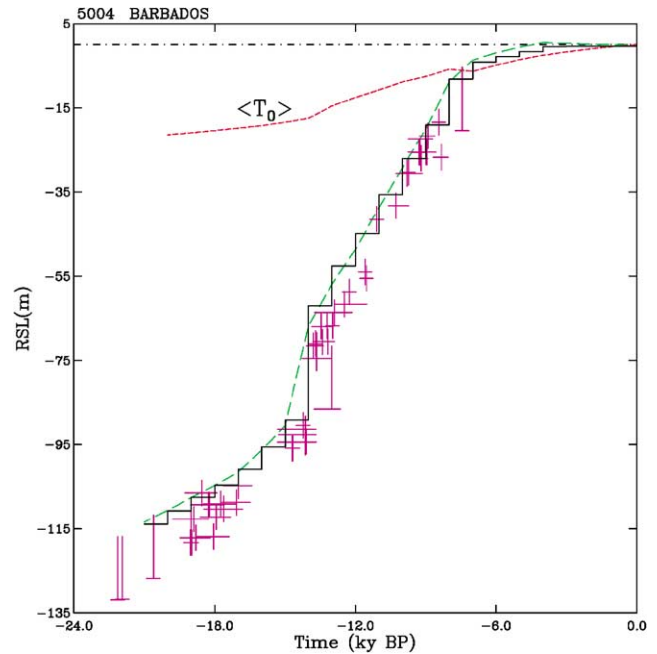

Fig. 3. The coral derived relative sea level record from Barbados of Fairbanks (1989) or the U–Th timescale of Bard et al. (1990a, b) is compared to the eustatic function of the theoretical model of the glacial isostatic adjustment process $S_{eus}(t)$ shown in Fig. 1a and to the RSL prediction for this location provided by the solution of the Sea Level Eq. (3) to obtain $S(\theta, \lambda, t)$. The eustatic function $S_{eus}(t)$ is the step-discontinuous curve whereas the smooth curve is the theoretical prediction $S(\theta, \lambda, t)$. The raw data from Barbados have been corrected for the influence of tectonic uplift by assuming an uplift rate of $0.39 \, \mathrm{mm \, yr^{-1}}$ as is conventional. The data represented by crosses are obtained from the shallow dwelling *Acropora palmata* species of coral and the vertical length of the segment corresponds to the maximum living depth correction of 6 m that is usually taken to be characteristic of this species in the modern local ecology. The data for which the vertical segment of the inverted T is longer are those derived from samples of the species *Porities* which may live at much greater depth below the surface of the sea than can *Acropora palmata*.

cannot therefore rule out the recent suggestion of Yokoyama et al. (2000) that an early meltwater pulse event near 19 ka could have led to a sharp rise of global sea level by an amount near 15 m at this time. However, given the extent to which the other Porities samples in the Barbados data set have been found to lie at a great depth below sea level (recall once more the sample of age near 13 ka) we would not advocate the existence of this event on the basis of the Barbados data set alone. To test the validity of the Yokoyama et al. (2000) conjecture we will need to seek observations from elsewhere.

Also shown explicitly in Fig. 3 is the time-dependent contribution $\langle T_o \rangle$ to the RSL history at Barbados. Since the contribution of this term to the predicted LGM depression of sea level at Barbados is approximately 20 m, the impact of this mass conservation term on the net eustatic depression is
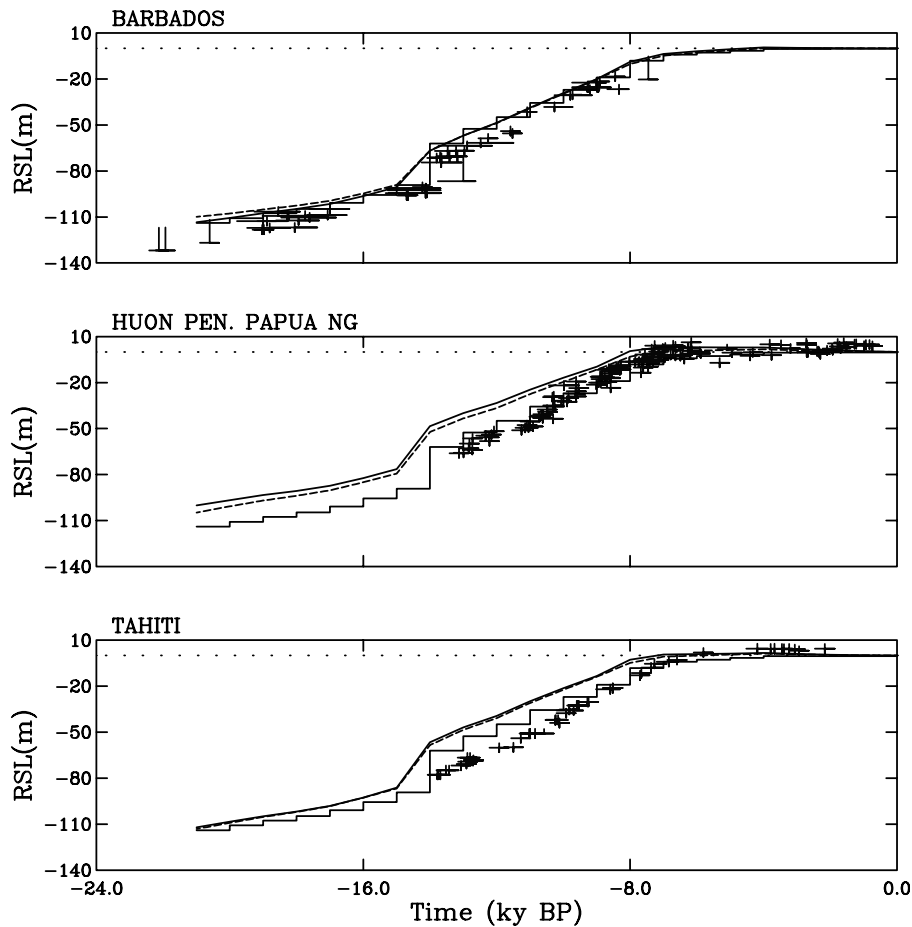
Fig. 4. Intercomparisons of the theoretical predictions of the model tuned to the Barbados coral derived record of RSL history shown in Fig. 2, repeated here as part (a) of the figure, to the (appropriately adjusted, see the text for discussion) coral derived records from (b) the Huon Peninsula of Papua, New Guinea (Chappell and Polack, 1991; Edwards et al., 1993) and from (c) Tahiti (Bard et al., 1996). The step discontinuous curves at each site correspond to the eustatic sea level history of the model from Fig. 1. The smooth curves are the predictions for each location based upon the solution of Eq. (3) neglecting the influence of rotational feedback. The dashed curves are predictions that include this influence.

approximately 16% and therefore extremely important. Since this contribution depends only upon time, it is the same at every point in space at which sea level history is predicted using this model. It will therefore not be necessary to explicitly plot this term at the other locations for which intercomparisons between RSL data and theoretical predictions will be provided in what follows.

4. (In) Validation of the global model of the GIA process that is tuned to the Barbados record of eustatic sea level history

Fig. 4 shows intercomparisons of the quality of the fit of the theoretical predictions to the data for Barbados as well as for two other sites from which additional long coral based records are available, namely from the Huon Peninsula using only data from Chappell and Polack (1991) and Edwards

et al. (1993), and from Tahiti (Bard et al., 1996). In plotting the data from these additional locations, I have assumed a maximum possible living depth correction of 6 m for the samples at both equatorial Pacific sites, which is in accord with the detailed analysis of the ecology of the modern species of corals that make up the assemblages sampled by the data set at the Tahiti location (Bard et al., 1996). For the purpose of plotting the data from the Huon Peninsula, furthermore, I have applied the usually assumed Pleistocene average correction for the influence of tectonic uplift of $1.9\,\mathrm{mm\,yr^{-1}}$ (Chappell and Polack, 1991), whereas at the Tahiti location I have employed the usually assumed correction for the influence of sea floor subsidence of $0.2\,\mathrm{mm\,yr^{-1}}$ (Bard et al., 1996). Inspection of the fits of the predictions of the Barbados tuned version of the theory to these additional data sets reveals that at both locations the misfit of the theoretical prediction to the observations is extremely large but that the misfit decreases
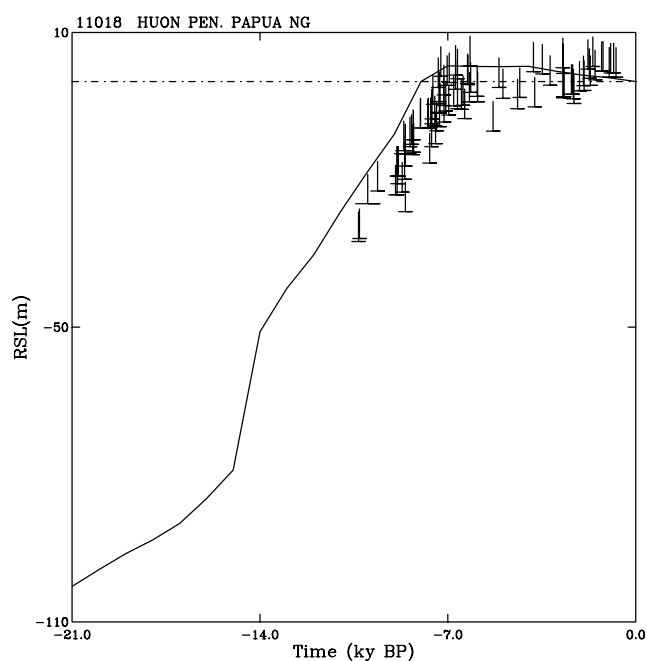
Fig. 5. Intercomparison of the theoretical predictions of the model tuned to the Barbados coral derived record of RSL history in Fig. 2, to the Holocene data from the Huon Peninsula of Papua, New Guinea of Chappell et al. (1996a, b), Ota et al. (1993) and Chappell et al. (1998). Individual data have been corrected for a rate of tectonic uplift based upon the assumptions that the eustatic sea level history of Fleming et al. (1998) is correct and that the data from the Huon Peninsula should record this history. It is argue in the text that neither of these assumptions is correct.

significantly with decreasing age of the individual coral specimens. In Peltier (1998a; see also the previously cited exchange of views between Edwards, 1995; Peltier, 1995) it was noted that essentially the entire misfit of the theory to the data from Huon was induced by the correction for the influence of tectonic uplift. This led to the suggestion that the problem at this site could be derivative of a flaw in the assumption that the Pleistocene average rate of tectonic uplift was equally applicable to the Holocene (see also Peltier, 1998d where this argument was repeated). In Fig. 26 of Peltier, 1998a it is shown that the entire misfit may be essentially eliminated simply by assuming that the Holocene rate of tectonic uplift was closer to $0.65\,\mathrm{mm\,yr^{-1}}$. There does exist the additional possibility, however, also suggested in Peltier (1998a), that the living depth correction at both the Huon and Tahiti sites, which is based upon the ecology of the modern coral assemblages at Tahiti, might not be appropriate for the same species which grew during the period of rapidly rising sea levels that characterized the early Holocene.

Fig. 5 provides some insight into the plausibility of the latter explanation for the misfits at Huon and Tahiti. In this figure I have plotted all of the available

Holocene data from sites along the coast of the Huon Peninsula (Ota et al., 1993, Chappell et al., 1996a, b, 1998). A maximum possible living depth correction of 6 m is assumed and the differing inferred rates of tectonic uplift thought to apply to each of the sampled locations has been invoked. It must be noted, however, that in Chappell et al. (1998) there is circularity of argument in the methodology employed to make the local estimate of uplift rate as the eustatic sea level curve of Fleming et al. (1998) was assumed to be valid (I will argue in what follows that this eustatic curve cannot be correct). Because the Fleming et al. (1998) eustatic curve posits a mid-Holocene-to-modern continuous rise of globally averaged sea level, the result of applying the local uplift rate correction to the Holocene data is to minimize or to entirely eliminate the mid-Holocene highstand of sea level that is so evident in the raw data (as discussed in Peltier, 1998a, d) and which is predicted by the Barbados tuned theoretical model. Since the mid-Holocene highstand of sea level is ubiquitous on islands through the equatorial Pacific ocean (sea further discussion to follow) any analysis which is designed to remove it from the raw data at any such location must been viewed as suspect. Taking this circularity of argument fully into account it is evident that, from approximately 10,000 years ago until the present, these more recently analysed Holocene data fit the predictions of the Barbados tuned theoretical model extremely well, especially as they are consistent, in the absence of the Fleming et al. (1998) based correction, with the existence of the mid-Holocene highstand of sea level with an amplitude of approximately 4 m at an age of approximately 4 ka that is predicted by the theory. Comparing the results of Fig. 5 to those in Fig. 4, it should be clear that a significant misfit between theory and observations at Huon therefore exists only for the earliest part of the record that begins only after mwp1a has ended. Furthermore, the magnitude of the misfit decreases continuously subsequent to the end of mwp1a, a property that is also characteristic of the misfit at the Tahiti location, as previously noted (see Fig. 4).

Since there are two records (Huon and Tahiti) which disagree with the late glacial and earliest Holocene predictions of the Barbados tuned version of the theory, in an essentially identical fashion (all three theoretical predictions together with all three observational data sets, with standard corrections applied, are shown colour coded together in Fig. 6 (the *Porites* samples from Barbados have been removed from this plot; also shown in this figure are the late glacial RSL data from the Sunda Shelf and J. Bonaparte Gulf to be discussed in what follows), one might be tempted to suggest that the theory should be tuned to the latter records (Huon and Tahiti) rather
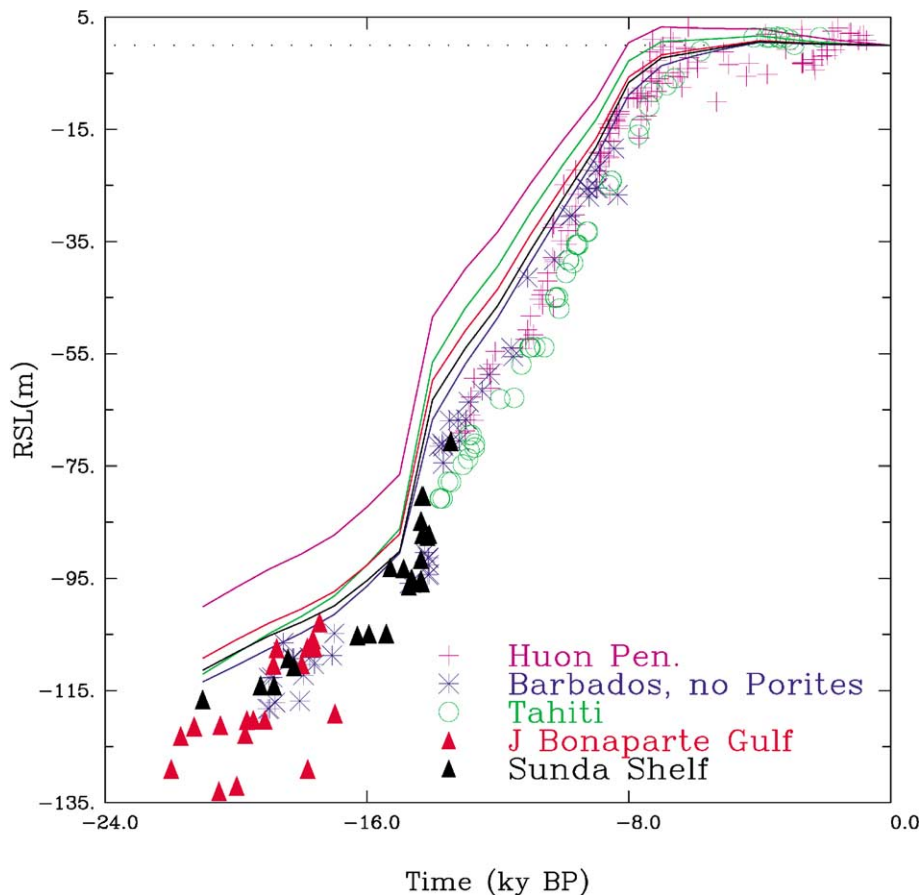
Fig. 6. Superposition of all of the coral derived RSL data from the three equatorial Pacific Ocean sites together with all of the theoretical predictions for the same locations. It will be noted that the RSL prediction of the Barbados tuned theoretical model of postglacial RSL history deviates most strongly from the observations at Tahiti and somewhat less strongly at the Huon, Peninsula.

than to the former (Barbados). Yet, as I have shown, a sea level record from Barbados of high accuracy would actually record ice-equivalent eustatic sea level history itself, or at least a good approximation thereto, and this record is unique in extending through the mwp1a event to LGM, implying that the *Acropora palmata* species of coral at this location was able to grow fast enough to track the rapidly rising level of the sea that occurred during the deglaciation event. It is nevertheless notable that the three coral based records, as conventionally corrected, are rather close to one-another (see Fig. 6), not withstanding the systematically increased depth of the Tahiti samples at all ages. This has led to the view that these records must be of similar quality as measures of ice-equivalent eustatic sea level history, which is in fact the case (excepting Tahiti) as demonstrated explicitly in Fig. 4, in each frame of which the step discontinuous eustatic curve is superimposed. The property which distinguishes the model data intercomparisons at Huon and Tahiti from that at Barbados is simply that at the former locations the theoretical prediction of RSL history is not expected

to be equivalent to the model eustatic history as the condition in $T_o = \langle T_o \rangle + S_{eus}^{im}$ does not obtain. Rather the prediction of the theoretical model of RSL history at each site lies well above sample depth, especially in the late glacial to early Holocene period. If we were to tune the model to Tahiti/Huon, we would therefore be obliged to employ a model of the deglaciation history characterized by a eustatic function which posits an LGM to Holocene eustatic rise of approximately 140 m (i.e., an increase from the nominal conventionally assumed LGM eustatic depression of 120 m by an amount equal to the LGM difference in depth between the theoretically predicted lowstand at either location and the eustatic function of the model). A model retuned in this way would clearly not fit the RSL record at Barbados. In the absence of further information one might be tempted to tune the model so as to best fit, in some least squares sense, the three coral based records collectively. This would clearly lead to a eustatic function characterized by an LGM lowstand intermediate between 120 and 140 m. It would not, however, allow for the distinct possibility that the Barbados record could be a superior measure of the LGM to

present ice-equivalent eustatic function than either of the other two.

It is very fortunate, therefore, that in the recent past a sequence of new records of early post LGM sea level history have become available that are not based upon corals. These records have all been obtained by sampling the sedimentary records on continental shelves which were originally significantly exposed at LGM (e.g. see Peltier, 1994 for graphics depicting many of the regions in which shelf exposure was extreme). The first of such records to appear was that for the tectonically stable Sunda Shelf, whose location is shown in Fig. 1, a record which was described by Hanebuth et al. (2000). This record is extremely important as it is significantly based upon ^{14}C dated samples of mangrove (the only exceptions among the 26 data points in this regard consist of the two oldest samples), which are exceptional sea level markers as they are invariably found in a sharply confined range within ~2 m of sea level (either at or as much as 2 m above this horizon). The record of Hanebuth et al. (2000) is compared in Fig. 7a to the theoretical predictions for this site based upon the global theoretical model of RSL history that is tuned to the Barbados record of eustatic sea level. Evident by inspection of the prediction shown as the black line is the fact that the theoretical model tuned to Barbados fits the Sunda Shelf record of Hanebuth et al. (2000) very precisely. All of the samples clustered near 14–15 kyr BP that record mwp1a, are mangrove (see Fig. 1 of Hanebuth et al., 2000). On this shelf, LGM sea level at 21 ka appears to have been depressed by an amount somewhat less than 120 m as assumed in the present model (the oldest dated sample, the age of which is near 22 ka, is at a depth of 116.6 m, but since this sample is not mangrove this means that sea level lay somewhat above this depth at LGM). Furthermore, this record explicitly captures the existence of the mwp1a event that was assumed to exist (but about which skepticism has been expressed as it was found to be coincident with a core-break; see however the recent paper by Sharma and Scott, 2001 in which the timing ascribed to mwp1a on the Sunda Shelf by Hanebuth et al., 2000 is questioned), in tuning the theory to the observations at Barbados. It is extremely important to note, furthermore, that the Hanebuth et al. (2000) record from the Sunda Shelf contains many samples in the age range near 19 ka and two samples of greater age which would appear to contradict the possibility of the significant additional sharp meltwater pulse induced eustatic rise at this time which Yokoyama et al. (2000) have hypothesized based upon their observations of RSL history from the continental shelf in J. Bonaparte Gulf. More data will be required to investigate this possibility more thoroughly and I do not therefore believe that this possibility has been ruled out. Also clear on the basis of inspection
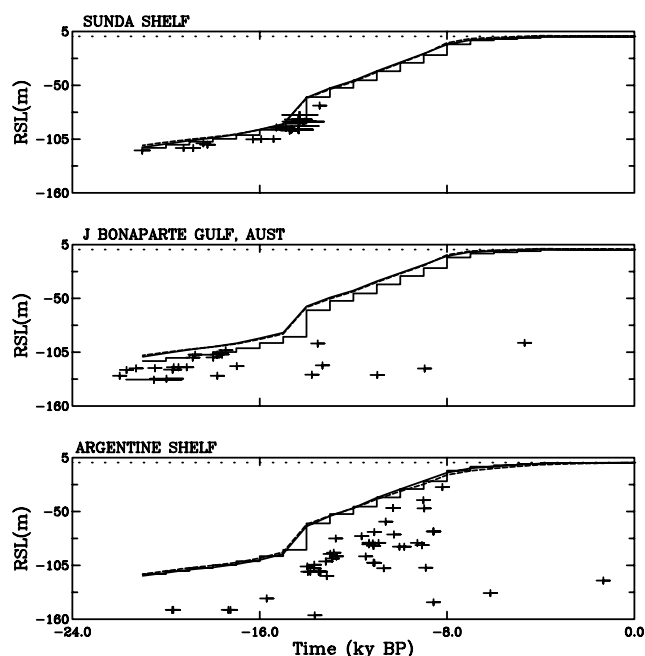

Fig. 7. Intercomparison of the observed histories of postglacial RSL variations obtained from continental shelf sediments from three locations, respectively the Sunda Shelf (Hanebuth et al., 2000), Bonaparte Gulf (Yokoyama et al., 2000) and from the Argentine Shelf (Guilderson et al., 2000), with the theoretical predictions of RSL history delivered by the Barbados tuned version of the theory. The grey curves shown in this figure are the predicted RSL histories at these sites made using a modified version of the SLE described in Peltier (2002) which treats the influence of up-shelf migration of the water load in a way that should be more accurate than the way in which this influence is treated in obtaining the standard predictions. The dashed curves for each location include the influence of rotational feedback whereas the smooth curves do not.

of this figure, if the black curves were an accurate prediction of RSL history, is that the Sunda Shelf record would also provide an excellent measurement of ice-equivalent eustatic sea level history itself, the step-discontinuous curve plotted in this figure representing the same eustatic function of the model as was compared to the observations at Barbados, Huon and Tahiti. Clearly then, if we were to tune the model by assuming a melting history that delivered a eustatic function which allowed us to fit the data from Huon and Tahiti we might not only grossly misfit the data from Barbados but also the RSL data from the Sunda Shelf (see, however, the further comments below concerning the interpretation of the red curves in Fig. 7).

Figs. 4 and 7, which respectively show intercomparisons of the theoretical predictions at the locations of the coral based records and the continental shelf based records, also show the difference between the theoretical predictions which neglect the influence of rotational feedback (solid curves) and those that include this influence (dashed curves). Clearly the importance of this feedback is minimal as previously

demonstrated (e.g. Peltier, 1999, 1998), insofar as relative sea level history is concerned. Its influence cannot therefore help to explain the difference in the quality of the fit between the predictions of the Barbados tuned theoretical model for the Sunda Shelf as opposed to Huon or Tahiti.

Two other continental shelf derived records, from the J. Bonaparte Gulf location off the coast of northern Australia (Yokoyama et al., 2000), and from the Argentine shelf off the east coast of South America (Guilderson et al., 2000), are also shown in Fig. 7, along with two versions (black and grey curves) of the RSL histories at these sites predicted by the theoretical model which was tuned to the Fairbanks (1989) and Bard et al. (1990a, b) record from Barbados. As these regions (the locations of which are also shown in Fig. 1), are also supposed to be fairly stable tectonically, no elevation corrections have been applied to the raw RSL estimates derived from them. The Yokoyama et al. (2000) record is especially important for the purpose of this discussion as it is the record which Clark and Mix (2000) have discussed as supporting of the notion that the LGM lowstand of eustatic sea level was located between 130 and 135 m below present sea level. Clearly, however, the raw data from the J. Bonaparte Gulf which are plotted in this figure appear to be consistent with the predictions of the Barbados tuned version of the theory (black curves) in that all of the immediately post LGM samples lie just below the predictions of the theoretical model (consistent with these samples having been derived on the basis of sub-sea-surface dwelling mollusks and foraminifers) at a depth very close to 120 m. It is important to recognize that the data of Yokoyama et al. (2000) are of significantly higher quality than those of Guilderson et al. (2000), however, as they derive from dated continental-marine transitions in cores from a coastal depression whereas Guilderson et al. (2000) dated individual marine shells found in unconsolidated marine sediments. In Yokoyama et al. (2000), the raw data plotted in Fig. 7 were, however, corrected by adjusting them in a way which the authors hoped would enable them to convert the locally determined RSL history so as to obtain what they refer to as "ice-equivalent" eustatic sea level history (compare Figs. 2a and b of Yokoyama et al., 2000; the raw data plotted in 2a are replotted in 2b by application of an ad hoc procedure). Lambeck and Johnston (2001) have now published a correction to the Yokoyama et al. (2000) paper in response to my having pointed out the flaw in their interpretation (this is discussed in greater detail in Peltier, 2002, this volume). The analyses presented herein show that the raw RSL observations at the far field Bonaparte Gulf location should also provide a very good approximation to ice equivalent eustatic sea level history if the theoretical

predictions for this site shown as the black curves were correct.

Also shown in Fig. 7 is the fit of the same theory to the data set recently collected from the Argentine shelf by Guilderson et al. (2000). This data set is based upon ^{14}C dating of the "shell hash" layers found in the suite of piston cores drilled from the Argentine shelf by Ewing and others in the 1960's and which are stored (!) at the Lamont Doherty Earth Observatory. Inspection of this record, from the high coastal energy (large amplitude tidal regime etc.) Argentine shelf, demonstrates that there is not only a considerable offset between theory and observations but that there is also considerable young material found at great depth. This observation implies that some (or all?) of the material on this continental shelf has been subjected to significant downslope movement from its original level of deposition. The contrast in the quality of this record and those from the Sunda Shelf and J. Bonaparte Gulf is therefore very apparent. The Sunda Shelf data set of Hanebuth et al. (2000) and the Bonaparte Gulf data set of Yokoyama et al. (2000) appear to be the best far field data sets available that may be invoked to constrain the magnitude of the RSL depression that obtained at LGM.

Returning to consideration of the coral based sea level records from the Huon Peninsula and from Tahiti, the situation is apparently that we now have two far field records which are not subject to the ambiguities of the coral derived records due to tectonics and living depth correction, both of which appear to be consistent with the Barbados tuned theory if the LGM lowstand is assumed to be near 120 m and if the theoretical predictions shown as the black curves on Fig. 7 are correct. The Huon and Tahiti records, however, appear to be in conflict. That this conflict may only be apparent, however, is also illustrated in Fig. 7 by the red curves. These additional theoretical predictions of relative sea level history at the three continental shelf locations have been produced using a further modified form of the SLE in which the upslope migration of the water load that occurs as sea level rises is treated in a way that is more accurate than that employed in the version of the theory that has been employed to this point (Peltier and Drummond, 2001). Although this modification to the SLE to better capture the impact on RSL history of continental shelf inundation has no significant effect at Barbados or Tahiti, it does potentially have a significant impact at the Sunda Shelf and J. Bonaparte Gulf locations. This impact is such as to induce a significant misfit between the local RSL history predicted by the theory and the eustatic function of the model. Furthermore, this misfit is very similar to that which exists at both Tahiti and the Huon Peninsula. To the extent that the modified treatment of RSL history in regions where a broad and initially exposed continental shelf is

inundated by the sea provides a stable estimate of this influence, we will be obliged to conclude that it may well be the RSL curve at Barbados that deserves to be questioned, rather than those at Tahiti and Huon. This would require us to accept the reality of a net LGM to present eustatic rise considerably greater than 120 m. The interested reader will find a very detailed discussion of this possibility in Peltier and Drummond (2001; see also Peltier, 2002, this volume).

5. Further comments on eustatic sea level history

Although our primary concern in this paper has been to infer a best estimate for the LGM lowstand of eustatic sea level, an analysis that has led us to suggest that the classical estimate of ~120 m may be a significant underestimate, it is also of interest, and of considerable importance, to constrain the form of the eustatic curve during the most recent Holocene epoch. Inspection of Fig. 1 will show that the eustatic curves characteristic of ICE-4G (VM2) - like models are characterized by the assumption that all continental ice sheet melting had effectively ceased by mid-Holocene time. In Fig. 1, the eustatic curve of the present model is characterized by a complete cessation of melting by 4 ka. Clearly there are very significant differences between the Fleming et al. (1998) model of eustatic RSL history and that recorded at Barbados to which the present model has been tuned. For example, the Fleming et al. eustatic sea level "conjecture" does not contain the mwp1a event, which seems to have been verified by the data from the Sunda Shelf which appear to explicitly resolve it and to reasonably confirm its timing. Secondly, however, the Fleming et al. eustatic curve also contains a late Holocene melting tail which they suggest could have been as strong as $0.5 \, \text{mm yr}^{-1}$ in terms of the sustained rate of eustatic sea level rise (in Fig. 2 of Chappell et al., 1998 the strength of the melting tail actually appears to be significantly stronger than this). As previously mentioned, the assumption of the validity of a eustatic curve with this property played a very significant role in the Chappell et al. (1998) reduction of the Holocene data from the Huon Peninsula, a reduction which amplifies the misfit of the data at this location to the predictions of the ICE-4G (VM2) theoretical model. This suggested property of the eustatic curve may be directly tested by simply adding a eustatic melting tail to the eustatic sea level history of any reasonable version of the ICE-4G (VM2) model, a history in which it has been assumed that all melting of land ice had ceased by 4 ka as demonstrated in Fig. 1. Fig. 8 illustrates the impact of the addition of melting tails of eustatic strength 0.25 and $0.50 \, \text{mm yr}^{-1}$ to the eustatic history shown in Fig. 1 in terms of the predicted present day rate of local RSL rise. Results are shown

for examples in which the melting tail is assumed to derive from either Greenland or Antarctica. For the strongest late Holocene melting tail of strength $0.5 \, \text{mm yr}^{-1}$, inspection of Fig. 8 shows that the sign of the predicted rate of RSL rise over the equatorial oceans is changed from negative (implying locally falling sea level) to positive (indicating locally rising sea level). This is because such intense late Holocene melting entirely eliminates the mid-Holocene highstand of sea level that is an observed characteristic of the record of RSL history at all equatorial Pacific Ocean locations and which is predicted by the model when all melting is assumed to cease by mid-Holocene time. Such highstand observations are shown for 16 of the island locations in Fig. 9a in Fig. 10, where RSL predictions for versions of the model with and without late Holocene melting are compared to the carefully quality controlled mid-Holocene highstand measurements of Grossman et al. (1998). Inspection of Fig. 10 will show that only the model with no late Holocene melting is able to fully reconcile the highstand observations. On this basis it therefore seems clear that the eustatic curve postulated by Fleming et al. (1998), which contains a significant late Holocene melting tail, is ruled out by the observations. Probably the most detailed observations of the equatorial highstand that are currently available at any such island location are those from the Fijian archipelago recently analysed in detail by Nunn and Peltier (2001). The totality of these data, together with the fit of the theoretical model to them, is shown in Fig. 9b, inspection of which will demonstrate the exceptional degree of definition of the highstand provided by the very large number of samples that make up the data set from this region. Also evident is the fact that the theoretical model of postglacial RSL history accurately predicts the amplitude and the timing of the highstand itself.

6. Conclusions

Based upon the analyses presented in the previous sections of this paper, the following tentative conclusions appear to be justified:

(1) Eustatic sea level at LGM was depressed below its present level by an amount that is well approximated by 120 m if the Barbados record of postglacial RSL history is assumed to be accurate and if the modified version of the SLE employed to predict the red RSL curves in Fig. 7 is over-estimating the impact of the up-shelf migration of the water level. Our analyses in fact allow us to refine the conventional estimate of the nominal eustatic depression somewhat. On the basis of
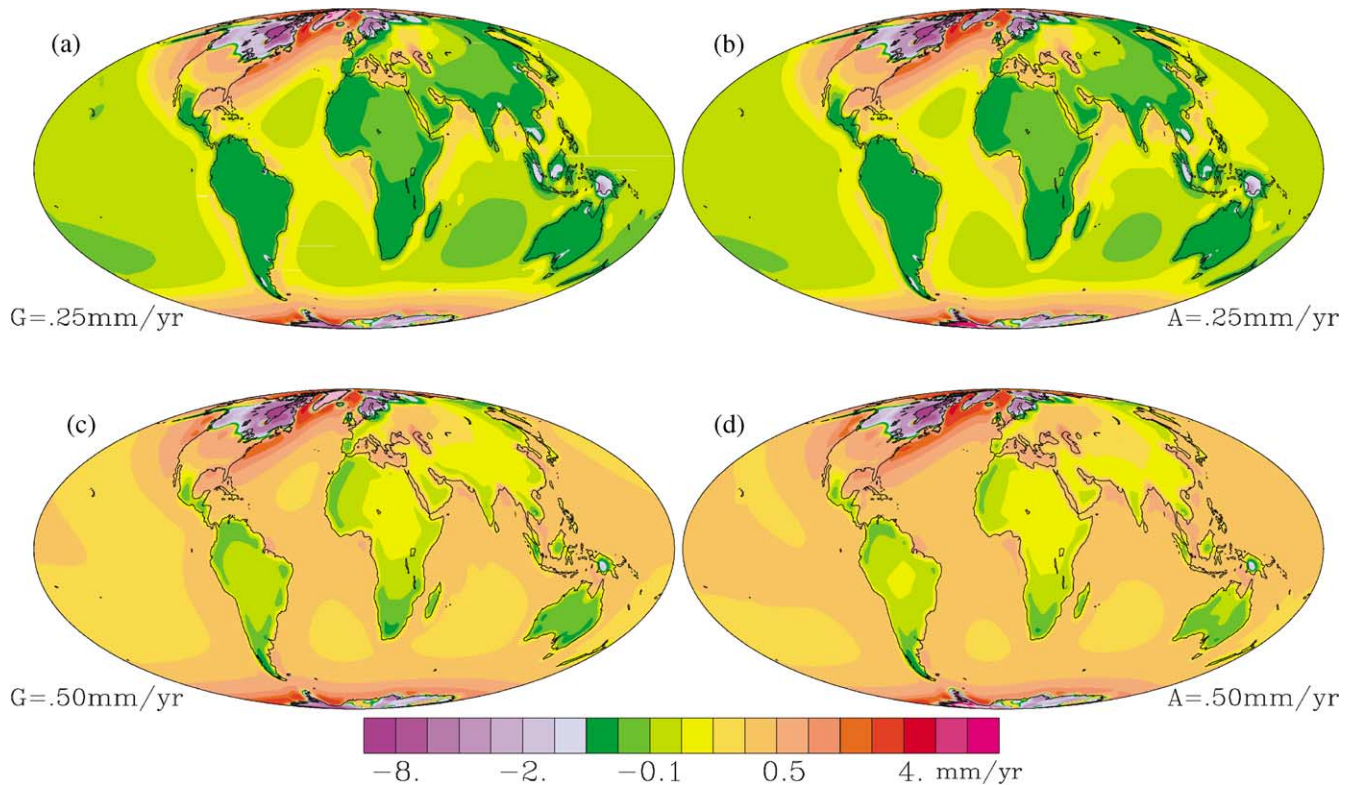
Fig. 8. Present day rates of RSL rise predicted by a modified version of the theoretical model of postglacial RSL history which differs from that whose eustatic function is shown in Fig. 1a in that late Holocene melting tails have been added, post 4 ka, of strength equal to either 0.25 or 0.50 mm yr^{-1}. The four different results correspond to those obtained when either melting tail is assumed to derive from Greenland or from Antarctica. Comparison of these results with those shown for the "tail free" version of the model in Fig. 1b demonstrates that the versions of the model which have the strongest late Holocene melting predict a reversal of the sign of the rate of change of RSL over the equatorial oceans. This is because the equatorial highstand of sea level is eliminated when such strong melting is assumed.

the Sunda Shelf data shown on Fig. 7 (using the unmodified version of the SLE), for example, the predicted RSL depression at LGM is essentially identical to the model eustatic depression of 113.5 m. Since the observed RSL depression at this site is 116.5 m, if we may assume the single old sample of age near 22 kyr to be accurate, this datum would fix the net LGM ice-equivalent eustatic depression to 116.5 m. On the basis of the J. Bonaparte Gulf data, however, it is notable that the model predicted RSL history is displaced somewhat from the eustatic curve of the model such that the latter lies at greater depth then the former at LGM. In order to bring the theoretically predicted LGM depression using the unmodified version of the SLE into accord with the observed LGM depression of 120 m, the eustatic curve of the model would have to be modified so as to add an additional 9.5 m to the sea level depression if the oldest samples at Bonaparte Gulf are assumed to record paleo sea level precisely. To the extent that these samples consist of sub-sea surface dwelling specimens, this represents an upper bound on the increase in the LGM eustatic

depression that must be added to the present model in order to satisfy the data. The upper bound on the LGM ice-equivalent eustatic depression of sea level suggested by the Bonaparte Gulf data is therefore 113.5 m + 9.5 m = 123 m. We might consider a best available upper bound estimate of the LGM eustatic depression to be the average of the constraints provided by the data from the Sunda Shelf and J. Bonaparte Gulf. This current best upper bound would then be (116.5 m + 123 m)/2 ≃ 120 m, essentially equal to the conventional estimate of 120 m based upon oxygen isotopes (see Shackleton, 2000) and entirely consistent with the original ICE-4G (VM2) model. If, however, we are obliged to accept the predictions of the modified version of the SLE for these two locations as being the more accurate, then we will also be obliged to accept a significantly higher value for the net eustatic rise (see Peltier and Drummond, 2001 and Peltier 2002, this issue for detailed discussion).

(2) Meltwater pulse 1a is a proven feature of postglacial eustatic sea level history

(3) In the period subsequent to 19 ka, the RSL record from the island of Barbados is an excellent proxy
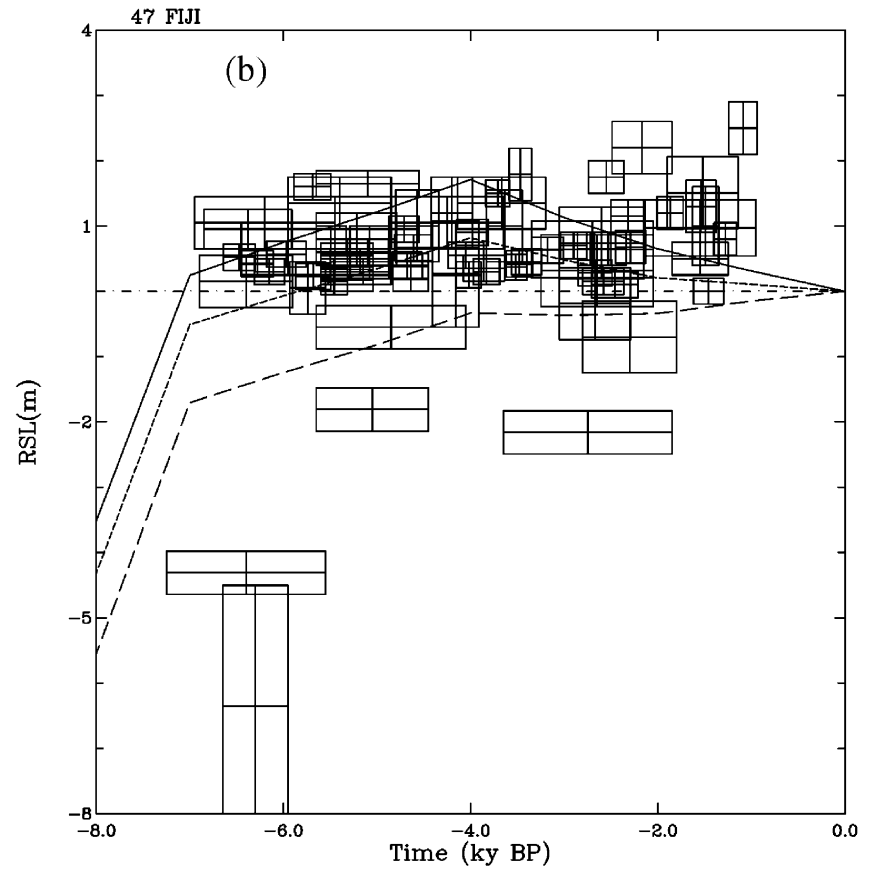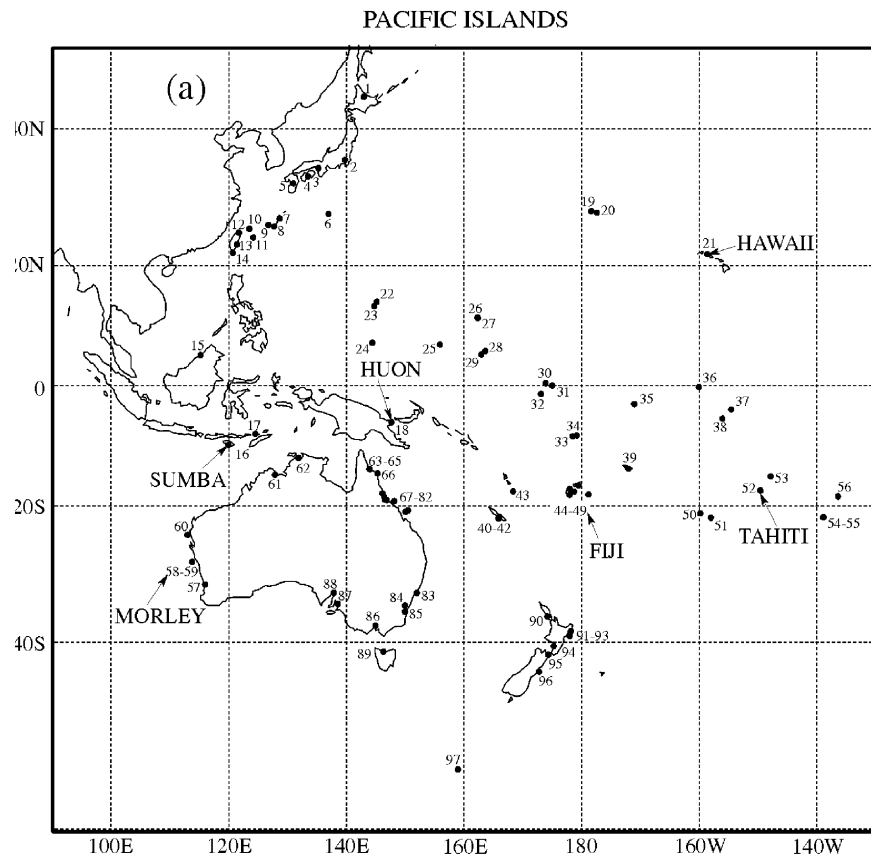
Fig. 9. (a) Location map for the islands in the Pacific Ocean from which mid-Holocene highstand observations are available, (b) Holocene RSL observations from the Fijian archipelago which define the mid-Holocene highstand very clearly (Nunn and Peltier, 2001) compared with the predictions of the Barbados tuned version of the theory which is characterized by a eustatic function in which all melting of land based ice ceased by 4 ka.
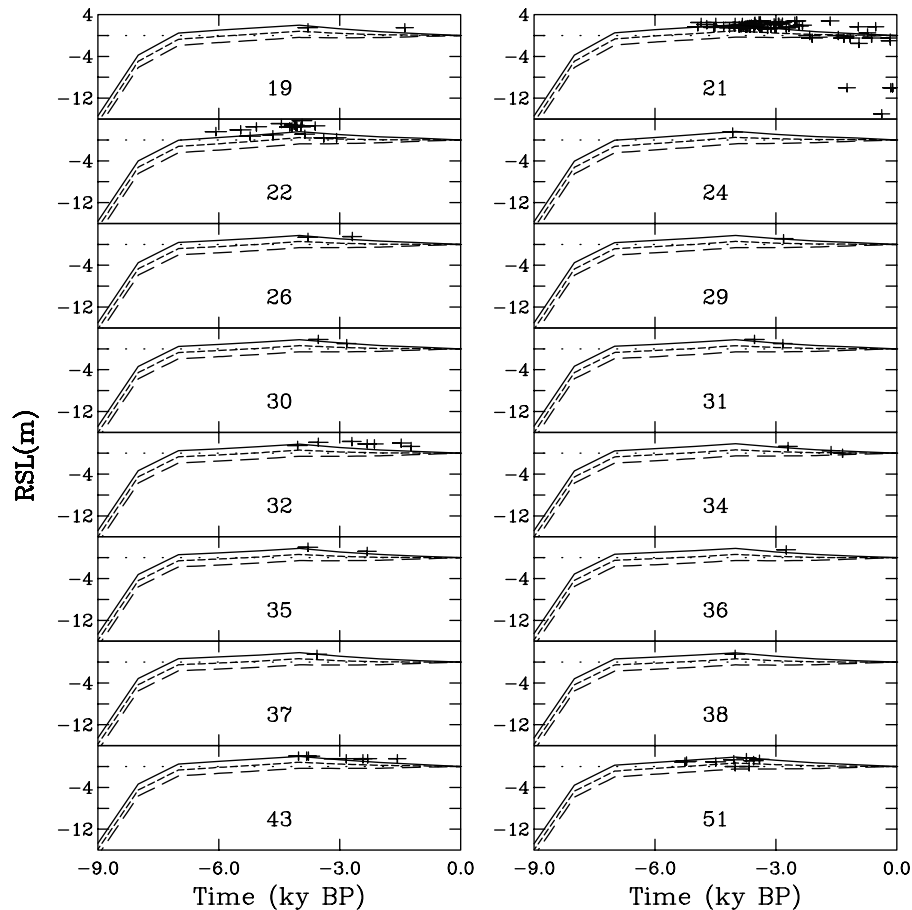
Fig. 10. Intercomparison of theoretical predictions of RSL history for models which both contain and do not contain late Holocene melting tails of strength 0.25 and 0.50 mm yr^{-1} based on the assumption that late melting is derived of Antarctica, together with the mid-Holocene highstand observations of Grossman et al. (1998). Results are shown for 16 of the Pacific Island locations that are numbered in Fig. 8a. The solid curves, which essentially perfectly fit the highstand observations at all locations, are those from the standard version of the model which has no late Holocene melting tail. The dotted and dashed curves are those for the models for which the strengths of the "melting tail" is 0.25 and 0.50 mm yr^{-1}. For the greatest tail strength it is clear that no mid-Holocene highstand is predicted at all.

for eustatic sea level itself, a fact that is only very weakly dependent upon the mantle viscosity profile employed in the global model of postglacial RSL history (see Peltier, 2002, this volume for an explicit demonstration of this fact).

(4) No significant degree of polar deglaciation could have been occurring continuously subsequent to approximately 4 ka. Although significant mass loss from the Greenland and Antarctic ice-sheet systems could have been occurring during the past century or so, this could not have persisted throughout late Holocene time, otherwise the well developed mid-Holocene highstand of sea level evident at far field locations would not exist.

I would be remiss in leaving the interested reader of this paper with the impression that I believe the ICE-4G (VM2) sequence of models to be exact and incontestable, even in detail, representations of the glacial isostatic adjustment process that has been

an ongoing characteristic of earth system dynamics since LGM. Indeed, examples exist in the current literature of misfits of these models to RSL observations in certain locations (Argus et al., 1999; Rostami et al., 2000; Morhange et al., 2001). These misfits clearly provide stimulus for further analyses which are ongoing and which will be reported upon in ensuing publications, one of which, that by Peltier and Drummond (2001), may be of particular interest in connection with the ideas discussed herein.

References

Argus, D.F., Peltier, W.R., Watkins, M.M., 1999. Glacial isostatic adjustment observed using very long baseline interferometry and satellite laser ranging geodesy. Journal of Geophysical Research 104, 29, 077–29, 093.

Bard, E., Hamelin, B., Fairbanks, R.G., Zindler, A., 1990a. Calibration of the ^{14}C timescale over the past 30,000 years using mass spectrometric U–Th ages from Barbados corals. Nature 345, 405–409.

Bard, E., Hamelin, B., Fairbanks, R.G., 1990b. U/Th ages obtained by mass spectrometry in corals from Barbados: sea level during the last 130,000 years. Nature 346, 456–458.

Bard, E., Hamelin, B., Arnold, M., Montaggioni, L., Cabioch, G., Faure, G., Rougerie, F., 1996. Deglacial sea level record from Tahiti corals and the timing of global meltwater discharge. Nature 382, 242–244.

Chappell, J., Polack, H.A., 1991. Post-glacial sea level rise from a coral record at Huon, Peninsula, Papua, New Guinea. Nature 276, 602–604.

Chappell, J., Omura, A., Esat, T., McCullock, M., Pandelfi, J., Ota, Y., Pillans, B., 1996a. Reconciliation of Late Quaternary sea levels derived from coral terraces at Huon Peninsula with deep sea oxygen isotope records. Earth and Planetary Science Letters 141, 227–236.

Chappell, J., Ota, Y., Berryman, 1996b. Late Quaternary coseismic uplift history of Huon Peninsula, Papua, New Guinea. Quaternary Science Review 15, 7–22.

Chappell, J., Ota, Y., Campbell, C., 1998. Decoupling post-glacial tectonism and eustasy at Huon Peninsula, Papua, New Guinea. In: Stewart, I., Vita-Finzi, C. (Eds.), Coastal Tectonics. Geological Society Special Publication No. 146.

Clark, P.U., Mix, A.C., 2000. Ice Sheets by Volume. Nature 406, 689–690.

Clark, J.A., Farrell, W.E., Peltier, W.R., 1978. Global changes in postglacial sea level: a numerical calculation. Quaternary Research 9, 265–287.

Dahlen, F.A., 1976. The passive influence of the oceans upon the rotation of the Earth. Geophysical Journal of the Royal Astronomical Society 46, 363–406.

Dyke, A.S., Prest, V.K., 1987. Late Wisconsian and Holocene history of the Laurentide Ice Sheet. Geogr. Phys. Quat. 41, 237–264.

Edwards, R.L., 1995. Paleotopography of Glacial-Age ice-sheets. Science 267, 536.

Edwards, R.L., Beck, J.W., Burr, G.S., Donhaue, D.J., Chappell, J.M.A., Bloom, A.L., Druffell, E.R.M., Taylor, F.W., 1993. A large drop in atmospheric $^{14}C/^{12}C$ and reduced melting in the Younger-Dryas documented with ^{230}Th ages of corals. Science 260, 962–968.

Fairbanks, R.G., 1989. A 17,000 year glacial eustatic sea level record: Influence of glacial melting rates on the Younger Dryas event and deep ocean circulation. Nature 342, 637–641.

Farrell, W.E., Clark, J.A., 1976. On postglacial sea level. Geophysical Journal of the Royal Astronomical Society 46, 647–667.

Fleming, K., Johnston, P., Zwartz, D., Yokoyama, Y., Lambeck, K., Chappell, J., 1998. Refining the eustatic sea level curve since Last Glacial Maximum using far-intermediate field sites. Earth and Planetary Science Letters 163, 327–342.

Guilderson, T.P., Burkle, L., Hemming, S., Peltier, W.R., 2000. Late Pleistocene sea level variations from the Argentine shelf, Geophysics, Geochemistry and Geosystems 1.

Grossman, E.E., Fletcher III, C.H., Richmond, B.M., 1998. The Holocene sea-level high stand in the equatorial Pacific: analysis of the insular paleosea-level data base. Coral Reefs 17, 309–327.

Hanebuth, T., Stattegger, K., Grootes, P.M., 2000. Rapid flooding of the Sunda Shelf: a late glacial sea level record. Science 288, 1033–1035.

Huybrechts, P., 1992. The Antarctic Ice Sheet during the last glacial-interglacial cycle: a three-dimensional experiment. Bericht Polarforschung 99, 1–241.

Huybrechts, P., 2001. Sea level changes at the LGM from ice-dynamic reconstructions of the Greenland and Antarctic ice sheets during the glacial cycles. Quaternary Science Review, in press.

Lambeck, K., Johnston, P., 2001. Correction to the paper "timing of the last glacial maximum from observed sea level minima. Nature, in press.

Milne, G.A., Mitrovica, J.X., 1996. Postglacial sea level change on a rotating Earth: first results from a gravitationally self-consistent sea level equation. Geophysical Journal International 126, F13–F20.

Morhange, C., Laborel, J., Hasnard, A., 2001. Changes of relative sea level during the past 5000 years in the ancient harbor of Marseilles, southern France. Palaeogeography Palaeoclimatology, Palaeoecology 166, 319–329.

Nunn, P.D., Peltier, W.R., 2001. Far-field test of the ICE-4G model of global isostatic response to deglaciation using empirical and theoretical Holocene sea-level reconstructions for the Fiji Islands, Southwestern Pacific, 2001. Quaternary Research 55, 203–214.

Ota, Y., Chappell, J., Kelley, R., Yonekura, N., Matsumoto, E., Nishimura, T., Head, J., 1993. Holocene coral reef terraces and coseismic uplift at Huon Peninsula, Papua, New Guinea. Quaternary Research 40, 177–188.

Peltier, W.R., 1974. The impulse response of a Maxwell Earth. Reviews of Geophysics Space Physics 12, 649–669.

Peltier, W.R., 1976. Glacial isostatic adjustment II: the inverse problem. Geophysical Journal of the Royal Astronomical Society 46, 669–706.

Peltier, W.R., 1994. Ice age paleotopography. Science 265, 195–201.

Peltier, W.R., 1995. Paleotopography of ice-age ice sheets. Science 267, 536–538.

Peltier, W.R., 1996. Mantle viscosity and ice-age ice sheet topography. Science 273, 1359–1364.

Peltier, W.R., 1998a. Postglacial variations in the level of the sea: implications for climate dynamics and solid earth geophysics. Review of Geophysics 36, 603–689.

Peltier, W.R., 1998b. "Implicit Ice" in the global theory of glacial isostatic adjustment. Geophysical Research Letters 25, 3957–3960.

Peltier, W.R., 1998c. The inverse problem for mantle viscosity. Inverse Problems 14, 441–478.

Peltier, W.R., 1998d. Global glacial isostatic adjustment and coastal tectonics. In Coastal Tectonics, Special Publication, No. 146, Geological Society of London, pp. 1–30.

Peltier, W.R., 1999. Global sea level rise and glacial isostatic adjustment. Global and Planet. Change 20, 93–123.

Peltier, W.R., 2002. Comments on the paper of Yokoyama et al. (2000) entitled "Timing of the Last Glacial Maximum from observed sea level minima". Quaternary Science Reviews 21 (this issue).

Peltier, W.R., Andrews, J.T., 1976. Glacial isostatic adjustment. I. The Forward problem. Geophysical Journal of the Royal Astronomical Society 46, 605–646.

Peltier, W.R., Drummond, R., 2001. A Broad Shelf effect upon postglacial Relative Sea Level history, Journal of Geophysical Research, submitted for publication.

Peltier, W.R., Solheim, L.P., 2001. Ice in the climate system: paleoclimatological perspectives. In: The present and future of climate modelling, T. Matsuno (Ed.), Book Containing the Proceedings of the 14th Toyota Conference, pp. 221–241.

Peltier, W.R., Farrell, W.E., Clark, J.A., 1978. Glacial isostasy and relative sea level: a global finite element model. Tectonophysics 50, 81–110.

Peltier, W.R., Shennan, I., Drummond, R., Horton, B., 2001. On the postglacial isostatic adjustment of the British Isles and the shallow viscoelastic structure of the Earth. Geophysical Journal International, in press.

Pinot, S., Ramstein, G., Harrison, S.P., Prentice, I.C., Guiot, J., Stute, M., Joussaume, S., 1999. Tropical paleoclimates at the Last Glacial Maximum: Comparison of Paleoclimate Modeling Intercomparison (PMIP) simulations and paleodata. Climate Dynamics 15, 857–874.

Rostami, K., Peltier, W.R., Mangini, A., 2000. Quaternary marine terraces, sea-level changes and uplift history of Patagonia,

Argentina: comparisons with predictions of the ICE-4G (VM2) model of the global process of glacial isostatic adjustment. Quaternary Science Review 19, 1495–1525.

Shackleton, N.J., 2000. The 100,000-year ice-age cycle identified and found to lag temperature, carbon-dioxide, and orbital eccentricity. Science 289, 1897–1902.

Sharma, C., David, B.S., 2001. The Sunda Shelf, South China Sea, during the late Quaternary: Sea level and flooding using foraminiferal evidence. PALAEO-3, submitted for publication.

Shennan, I., Peltier, W.R., Drummond, R., Horton, B., 2002. Global to local scale parameters determining relative sea-level changes and postglacial isostatic adjustment of Greater Britain. Quaternary Science Review 21 (this issue).

Tarasov, L., Peltier, W.R., 2001. Greenland glacial history and local geodynamic consequences, Geophysical Journal International, submitted for publication.

Vettoretti, G., Peltier, W.R., McFarlane, N.A., 2000. Global water balance and atmospheric water vapour transport at last glacial maximum: climate simulations with the Canadian climate centre for modelling and analysis atmospheric general circulation model. Canadian Journal of Earth Science 37, 695–723.

Yokoyama, Y., Lambeck, K., De Dekkar, P., Johnston, P., Fifield, L.K., 2000. Timing of the last glacial maximum from observed sea-level minima. Nature 406, 713–716.